

ONLINE EXTENDED METHODS

Reagents

AC220 (HY-13001), CB839 (HY-12248) and Phenformin (HY-16397A) were purchased from Insight Biotechnology. L-Buthionine-(S,R)-Sulfoximine (B2515), N-Acetyl-Cysteine (A9165), dimethyl 2-oxoglutarate (349631), L-Aspartic acid (A9256) and sodium pyruvate (S8636) were purchased from Sigma. TRIPZ Inducible Lentiviral GLS shRNA vector was obtained from Dharmacon.

Generation of genome-wide mutant libraries and screening

CRISPR screens were performed using the previously reported Wellcome Trust Sanger genome-wide CRISPR library¹. 3.0×10^7 cells were infected with a pre-determined volume of the genome-wide gRNA lentiviral supernatant that gave rise to 30% transduction efficiency measured by BFP expression. Two independent infections were conducted for the human AML cell line MOLM13. Two days after transduction, the cells were selected with puromycin at $1.5 \mu\text{g ml}^{-1}$. On day 15 post-transduction, cells were treated with either DMSO or IC_{50} of AC220 for the 3 following days and the media replaced with fresh without any drug supplement. On day 30, cells were pulled per condition and genomic DNA extraction was performed.

Illumina sequencing of gRNAs and statistical analysis

Genomic DNA extraction and Illumina sequencing of gRNAs were conducted as described previously. For the MOLM13 cells, 19-bp single-end sequencing was performed with the custom sequencing primer 5'-TCTTCCGATCTCTTGTGGAAAGGACGAAACACCG-3'. The numbers of reads for each guide were counted with an in-house script. Enrichment and depletion of guides and genes were analysed using MAGeCK statistical package by comparing read counts from the DMSO condition (Day 30) with counts from the AC220 condition (Day 30). Target genes for further analysis were selected based on having at least

80% of their targeting gRNA depleted >0.5 fold change (\log_2) with FDR <0.01. Only gRNA with at least 30 reads in the DMSO control were used for this analysis.

Lentivirus production and transduction

For shRNA, TransIT-LT1 transfection reagent (Mirus) was used to transfect the TRIPZ Inducible Lentiviral GLS shRNA vector (Dharmacon) and the packaging plasmids pMD2G and psPAX2 into 293T cells according to the manufacturer's protocol. Lentiviral supernatants were collected at 48 and 60 h after transfection. Cells were then spinoculated with lentiviral supernatant supplemented with Polybrene 4 μ g/ml (Sigma) at 32°C, 2500RPM, for 90 minutes on 2 consecutive days. After that, the medium was refreshed and cells cultured further. For CRISPR/Cas9, lentiviral particles were produced as described previously for the human and mouse AML cells¹. 1×10^6 cells and viral supernatant were mixed in 2 ml of culture medium supplemented with 8 μ g ml⁻¹ (human) or 4 μ g ml⁻¹ (mouse) polybrene (Millipore), followed by spinfection (60 min, 900 g, 32 °C) and further incubated overnight at 37 °C. The medium was refreshed on the following day and the transduced cells were cultured further.

gRNA competition assays

gRNA competition assays were performed using single and dual gRNA vectors as described previously¹. For the validation of individual target genes, one gRNA was derived from the CRISPR library used in the screens and another gRNA was designed using <http://www.sanger.ac.uk/htgt/wge/>. Viral supernatants were collected 48 h after transfection. All transfections and viral collections were performed in 24-well plates and transduction was performed as mentioned above. For gRNA/BFP competition assays, flow cytometry analysis was performed on 96-well plates using a LSR Fortessa instrument (BD). Gating was performed on live cells using forward and side scatter, before measuring of BFP⁺ cells. The gRNA sequences are listed below.

Cell Proliferation Assays

Cells were plated for 72h with indicated concentrations of inhibitors and proliferation measured using CellTiter 96 AQueous Non-Radioactive Cell Proliferation Assay (Promega).

Flow cytometry analyses (including apoptosis, ROS, TMRM and Mitotracker assays)

For apoptosis assay around 1×10^6 cells per condition were washed with PBS and stained using Annexin V and 7AAD (BD Biosciences) as per manufacturer protocol. Briefly cells were washed and resuspended in 100 μ L of annexin binding buffer (BD Biosciences) containing 5 μ L each of Annexin V antibody and 7AAD. Following 15 minutes incubation in the dark, further 400 μ L of annexin binding buffer were added to each sample and the sample were immediately analysed using LSR Fortessa (BD) instruments. For *in vivo* experiments, bone marrow and spleen single cell suspension were stained with anti-human CD45 FITC and anti-mouse CD45 APC antibodies (BioLegend) for 30 minutes on ice and then washed and analysed using LSR Fortessa (BD) instruments. For ROS, TMRM and Mitotracker analyses, cells were washed and stained with respectively CellRox® Deep red probe (Life Technologies, 500nM) which specifically measure cytoplasmic intracellular ROS, Tetramethylrhodamine (TMRM, Invitrogen, 20nM) and Mitotracker (Invitrogen, 25nM) and analysed as per manufacturer protocol.

Western blot analysis

Cell pellets were resuspended in either whole cell lysis buffer (50 mM Tris-HCl pH=8, 450 mM NaCl, 0.1% NP-40, 1mM EDTA), supplemented with 1 mM DTT, protease inhibitors (Sigma), and phosphatase inhibitors (Sigma) or equal number of cells were directly lysed in Laemmli buffer prior to loading. For samples lysed in whole cell lysis buffer, protein concentration was assessed by Bradford assay (Bio-Rad) and an equal amount of protein was loaded per lane. Prior to loading, the samples were supplemented with SDS-PAGE sample buffer, when necessary. Protein lysates were separated on SDS-PAGE gels, and blotted onto polyvinylidene difluoride (PVDF) membranes (Millipore). PVDF membranes were incubated with the relevant primary antibody and corresponding secondary antibodies

and images processed and acquired using LI-COR Odyssey System. Primary antibodies used were: KGA/GAC rabbit polyclonal antibody (Proteintech, cat no. 12855-1-AP), GAPDH mouse monoclonal antibody (Abcam, cat no.9484), Actin rabbit polyclonal (Abcam, cat no.8227).

Quantitative RT-PCR (qPCR)

Total RNA was isolated using the RNeasy Mini Kit (Qiagen). For cDNA synthesis, total RNA was reverse-transcribed with SuperScript™ III First-Strand Synthesis System (Invitrogen, 18080051) and qPCR reactions were performed using Brilliant III Ultra-Fast SYBR Green QPCR Master Mix (Agilent Technologies, 600882) on a Stratagene MX 3000P qPCR system and data were analyzed using MXPro v4.10 software (Stratagene). Primer sequences are provided below.

Extracellular flux profiling

Oxygen consumption rate (OCR) and Extracellular acidification rate (ECAR) levels were determined using a Seahorse XF^e24 analyser (cell lines) and Seahorse XF96 (primary AML samples). Following culture in their appropriate media and experimental conditions, 0.15-0.3 x 10⁶ cells were resuspended in bicarbonate-free RPMI (Sigma) with no FBS (cell lines) and 1% FBS (primary cells) and, where appropriate, 11 mM Glucose, 2 mM L-glutamine, pH 7.4, attached to Seahorse plates previously coated with Cell-Tak (Corning, 354240) and incubated at 37 °C for 30 min in a CO₂-free incubator prior to analysis. Each cycle of measurement involved 2 min mixing, 2 min waiting and 3 min measuring. After baseline measurements, testing agent prepared in assay medium was injected and followed by subsequent measuring cycles. Glycolysis stress test was performed as follows: measurement 1–3, basal (no glucose); 4–6, glucose (10 mM); 7–9, complex V inhibitor oligomycin (1 μM); and 10–12, 2-deoxyglucose (2DG, 50 mM) (note for primary samples and additional step with Carbonyl cyanide 4-(trifluoromethoxy)phenylhydrazone (FCCP) 500nM was added following oligomycin). Mitochondrial stress test: measurement 1–3, normal

(basal + 11 mM glucose); 4–6, oligomycin (1 μ M); 7–9, carbonyl cyanide *m*-chlorophenylhydrazone (FCCP, 300 nM); and 10–12, antimycin (1 μ M). DNA content (CyQuant cell proliferation assay, Thermo Fisher) protein content (BCA assay, Thermo Fisher) at endpoint or cell number was used for data normalization as specified.

Glucose/Glutamine uptake analysis and GSH/GSSG measurement

Glucose and glutamine from spent media of MV411 and MOLM13 cells were measured via automated spectrophotometric assays using respectively a Siemens Dimension EXL and a Randox Daytona⁺ autoanalyser. GSH/GSSG levels were calculated using the GSH/GSSG-Glo™ Promega kit (V6611).

Sample preparation and liquid chromatography coupled to mass spectrometry (LC-MS) for metabolomics analysis

MV411 cells were plated at 0.5×10^6 cells per mL in media supplemented with U-¹³C₆-glucose (11 mM) or U-¹³C₅, ¹⁵N₂-glutamine (2 mM) (Cambridge Isotope laboratories) for 48 h before sampling. Metabolites were extracted from cell-conditioned medium (extracellular) and cell pellets (intracellular) in 50% methanol: 30% acetonitrile: 20% H₂O with 100 ng ml⁻¹ HEPES buffer (100 μ l per 4×10^6 cells). Samples were incubated on dry-ice and methanol for 15 min and then at 4 °C for 15 min at 1500 r.p.m. on a thermomixer, before centrifugation at 13,000 r.p.m. (15,700g). Supernatant was transferred to vials for liquid chromatography coupled to mass spectrometry (LC-MS) analysis.

LC-MS analysis of sample extracts was performed on a Q Exactive mass spectrometer coupled to Dionex UltiMate 3000 Rapid Separation LC system (both Thermo Fisher Scientific). The liquid chromatography system was fitted with a SeQuant ZIC-pHILIC (150 mm \times 2.1 mm, 5 μ m) with guard column (20 mm \times 2.1 mm, 5 μ m) from Merck (Darmstadt, Germany), and temperature maintained at 30°C. The mobile phase was composed of 20mM ammonium carbonate and 0.1% ammonium hydroxide in water (solvent A), and acetonitrile (solvent B). The chromatographic gradient was run at flow rate of 180 μ L \times min⁻¹ as follows:

0-1 min: hold at 70% B; 1-16 min: linear gradient from 70% to 38% B; 16-16.5 min: linear gradient from 38% to 70% B; 16.5-25 min: hold at 70% B. The mass spectrometer was operated in full MS and polarity switching mode. The samples key was unknown to the operator, and samples were randomised in order to avoid bias due to machine drift. The acquired spectra were analysed using XCalibur Qual Browser and XCalibur Quan Browser software (Thermo Fisher Scientific) by referencing to an internal library of compounds.

FLT3^{ITD} variant allele frequency measurement

Individual NGS libraries were generated starting from 25ng of DNA using the following primer sequences: Forward: 5'-GCAATTTAGGTATGAAAGCCAGC-3', Reverse: 5'-CTTTCAGCATTTTGACGGCAACC-3'. Libraries were pooled and ran on a MiSeq. In order to detect insertions and deletions in the PCR amplified region of gene FLT3, pair-end reads were merged into one read using Paired-End reAd mergeR (PEAR)-0.9.6 (<http://www.exelixis-lab.org/web/software/pear>)². The unique merged reads were counted and their frequency and length compared to human reference genome obtained from Ensembl (www.ensembl.org). Reads with no alignment to FLT3 were discarded. Fully aligned reads and reads with the most frequent inserted region were counted as wild type and the main FLT3^{ITD} mutated variant, respectively. The variant allele frequencies (VAF) were calculated by dividing the number of these mutated reads on the total reads count.

RNA-seq analysis and GSEA analysis

The RNA-seq data for MV411, MOLM13 and K562 cells treated for 18 hours with DMSO or 1nM AC220 (MV411 and MOLM13) and 2μM Imatinib (K562) were generated as biological duplicates. RNA was isolated using RNeasy Mini Kit (Qiagen) with genomic DNA depletion. Ribosomal RNA was removed using Ribo-Zero rRNA Removal Kit (Human/Mouse/Rat) (Illumina), and library produced using the dUTP directional method using NEXTflex Rapid Directional RNA-Seq Kit (Bioo Scientific) and sequenced using HiSeq 4000 system (Illumina). The 150 bp paired-end Illumina reads were aligned to human genome (UCSC

hg19) using RNA-seq aligner STAR (version 2.4.0)³ and the number of uniquely mapped reads were estimated using HTSeq-Count⁴. DESeq2 (version 1.12.4)⁵ was used to identify differentially expressed genes after filtering genes with low read counts. Genes with adjusted P value <0.01 and fold change (\log_2) >0.5 were considered having a significant altered expression. The gene signatures used for Volcano Plot were generated by the authors based on published KEGG, BIOCARTA and REACTOME curated gene sets and are listed in Supplemental tables. GSEA analysis of published datasets was carried out using the Broad Institute software (<http://software.broadinstitute.org/gsea/index.jsp>)^{6,7}. Genes were ranked using the signal-to-noise metric and FDR and NES were calculated using gene-set permutation.

Statistics

Data were visualized and statistical analyses performed using Prism 6.0 software (Graph Pad). P values < 0.05 were considered to be statistically significant. Statistical tests used are outlined in figure legends. Error bars are mean \pm standard error of mean (s.e.m.).

Datasets

RNA-seq data are available under accession number GSE105161

Study approval

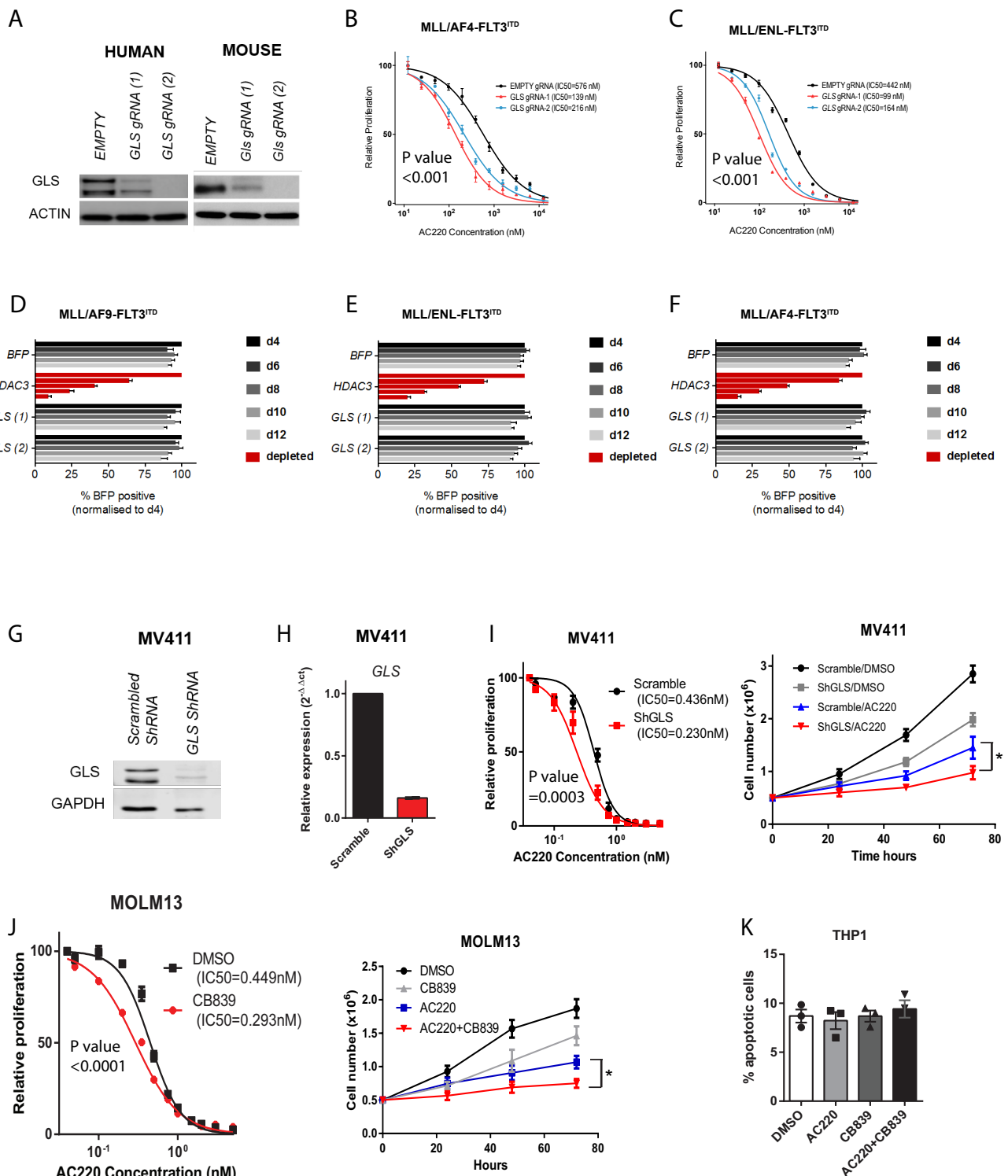
All animal experiments complied with local and national regulations and were performed under an existing UK Home Office project licence (PA46C00DB). Primary human samples were obtained after taking informed consent in accordance with the Declaration of Helsinki and the study was conducted under local ethical approval (REC 07-MRE05-44).

| gRNA competition assay | |
|------------------------|----------------------|
| Human gRNAs | Sequence |
| <i>GLS</i> (1) | GCTCCGAAGGAGAGCTGGAC |
| <i>GLS</i> (2) | GAGCACGCATCCGCAGCCCG |
| <i>HDAC3</i> | GGTAATGCAGGACCAGGCTA |
| Mouse gRNAs | Sequence |
| <i>Gls</i> (1) | GCAACTCACTTGTGCGCCCG |
| <i>Gls</i> (2) | GCTCCTGTAGGATCTCCGA |
| <i>Hdac3</i> | TTCCTGAACCCCGTCACCA |

| | q-PCR (human primers) | |
|---------------|-----------------------|-------------------------|
| | Forward Primer | Reverse Primer |
| <i>GLS</i> | CGATTTGTGGGGTGTGTCTG | ATCGATGCACATATTCAGTTCCA |
| <i>GLUD1</i> | TGTGCAGTGGTTGATGTGC | CACATCAATGCCAGGACCAA |
| <i>LDHA</i> | CAGCCCGATTCCGTTACCTA | TGGGTGCAGAGTCTTCAGAG |
| <i>GLUT3</i> | CTAAGCAGATCCTCCAGCGG | TGATGATGGGCTGTGCGGTAG |
| <i>GCLC</i> | CAGGTGACATTCCAAGCCTG | AATCACTCCCCAGCGACAAT |
| <i>NFE2L2</i> | TGCCCACATTCCCAAATCAG | ACTGGGCTCTCGATGTGAC |
| <i>PC</i> | TGGCCAAGGAGAACAACGTA | CCTCCACCTTGTCTCCCATC |
| <i>PDHA1</i> | AGGAGGATCGATGCACATGT | GCAGCACCATCGCCATATAA |
| <i>PDHB</i> | AGAGATGGGCTTTGCTGGAA | TGAAGGCCACCAGACATGTA |
| <i>B2M</i> | ACTGAATTCACCCCCACTGA | TGGAATTCATCCAATCCAAA |

SUPPLEMENTAL DATA REFERENCES

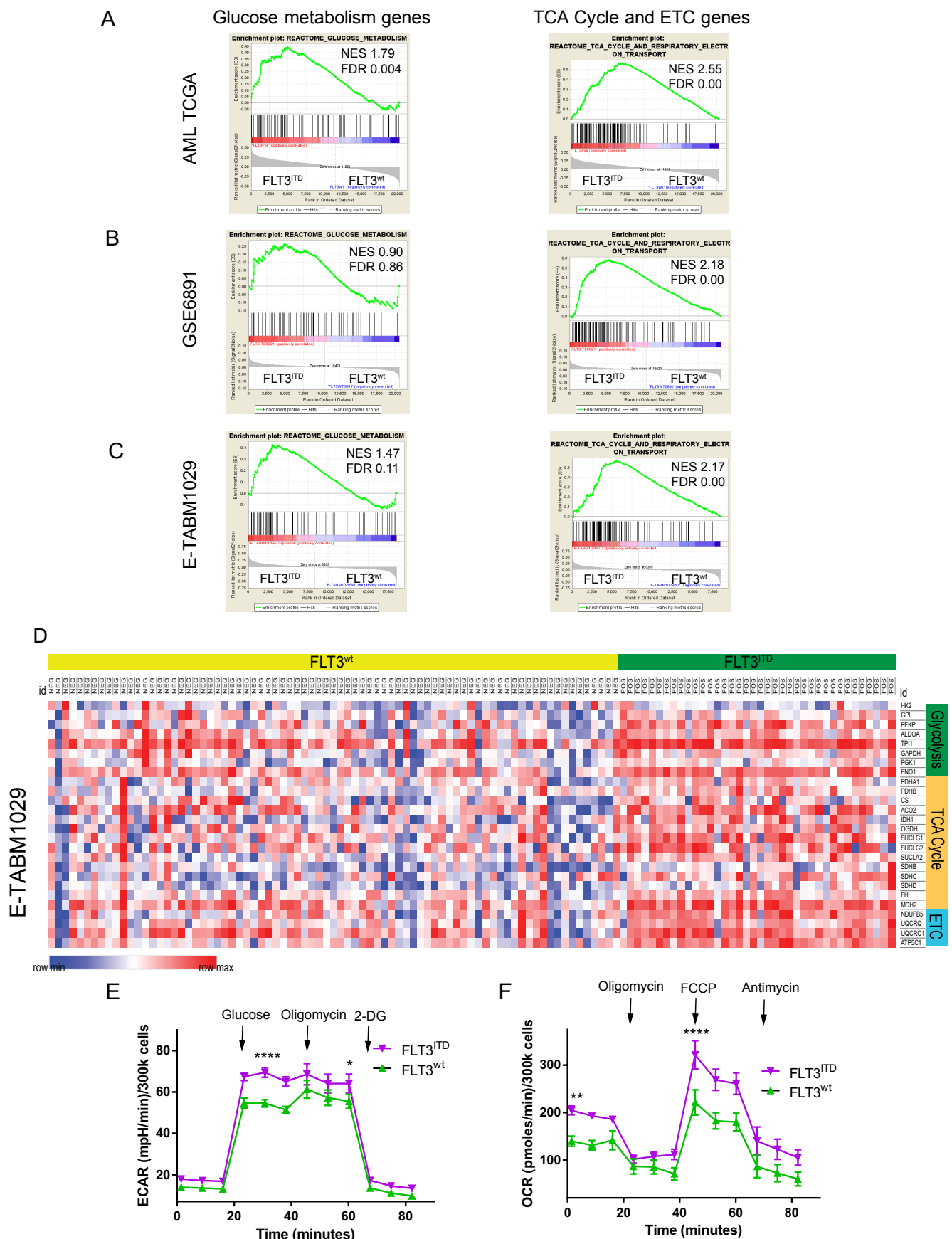
1. Tzelepis K, Koike-Yusa H, De Braekeleer E, et al. A CRISPR Dropout Screen Identifies Genetic Vulnerabilities and Therapeutic Targets in Acute Myeloid Leukemia. *Cell Rep.* 2016;17(4):1193-1205.
2. Zhang J, Kobert K, Flouri T, Stamatakis A. PEAR: a fast and accurate Illumina Paired-End reAd mergeR. *Bioinformatics.* 2014;30(5):614-620.
3. Dobin A, Davis CA, Schlesinger F, et al. STAR: ultrafast universal RNA-seq aligner. *Bioinformatics.* 2013;29(1):15-21.
4. Anders S, Pyl PT, Huber W. HTSeq--a Python framework to work with high-throughput sequencing data. *Bioinformatics.* 2015;31(2):166-169.
5. Love MI, Huber W, Anders S. Moderated estimation of fold change and dispersion for RNA-seq data with DESeq2. *Genome Biol.* 2014;15(12):550.
6. Subramanian A, Tamayo P, Mootha VK, et al. Gene set enrichment analysis: a knowledge-based approach for interpreting genome-wide expression profiles. *Proc Natl Acad Sci U S A.* 2005;102(43):15545-15550.
7. Mootha VK, Lindgren CM, Eriksson KF, et al. PGC-1alpha-responsive genes involved in oxidative phosphorylation are coordinately downregulated in human diabetes. *Nat Genet.* 2003;34(3):267-273.



Supplemental Figure 1

Supplemental Figure 1 (Related to Figure 1): Extended results of *GLS* gene deletion and chemical inhibition in combination with AC220 on FLT3^{ITD} mutated AML cells

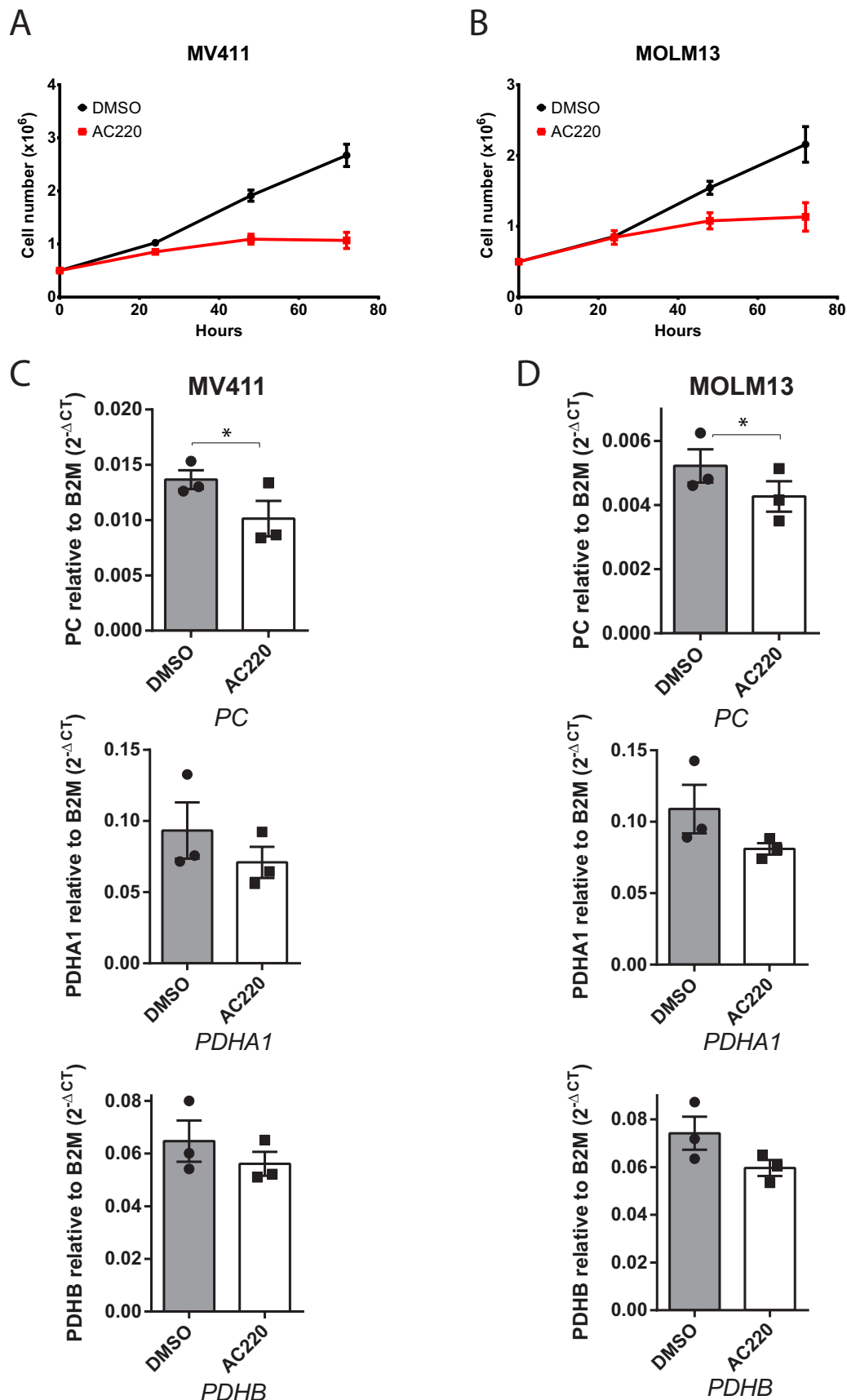
(A) Western blot showing protein depletion following transduction of gRNA targeting respectively human *GLS* (both kidney (K-type) glutaminase (KGA, top) and glutaminase C (GAC, bottom) isoforms encoded by human *GLS*, are shown as depleted) and mouse *Gls*. **(B-C)** Growth inhibition curves to AC220 of murine bone marrow cells expressing MLL/AF4-FLT3^{ITD} **(B)** and MLL/ENL-FLT3^{ITD} **(C)** transduced respectively with “empty” gRNA control or 2 different gRNA targeting *Gls* (mean ± s.e.m., n=3, P<0.001 for treatment effect comparing control and both *Gls* knockout, two-way ANOVA). **(D-F)** Competitive co-culture of lentiviral *Gls* gRNA-transfected (Blue Fluorescent Protein, BFP positive) vs untransfected FLT3^{ITD} mutated AML cells normalized to %BFP on day 4 (mean ± s.e.m., n=3). **(G-H)** Western blot and q-PCR showing depletion of protein **(G)**, both isoforms encoded by human *GLS* are shown as before) and mRNA levels **(H)** in MV411 cells lentivirally transduced with control “Scramble” shRNA and *GLS* shRNA. **(I)** Growth inhibition curves to AC220 of MV411 transduced respectively with control “Scramble” shRNA and *GLS* shRNA (mean ± s.e.m., n=3) (left panel, P=0.0003 for treatment effect, two-way ANOVA) and proliferation of Scramble and shRNA transduced cells treated with AC220 0.5nM (mean ± s.e.m., n=14, * P=0.0155, two-way ANOVA with Bonferroni’s multiple comparisons) (right panel). **(J)** Growth inhibition curves to AC220 of MOLM13 cells treated with respectively CB839 at 100nM and vehicle control (left panel, P<0.0001 for treatment effect, two-way ANOVA) and proliferation of cells treated AC220 1nM, CB839 100nM or their combination (mean ± s.e.m., n=11, * P=0.0334, two-way ANOVA with Bonferroni’s multiple comparisons). **(K)** Apoptosis in the FLT3^{WT} cell line THP1 following treatment with AC220 1nM, CB839 100nM or their combination (mean ± s.e.m., n=3).



Supplemental Figure 2

Supplemental Figure 2 (Related to Figure 2): FLT3^{ITD} mutated AML displays enhanced central carbon metabolism

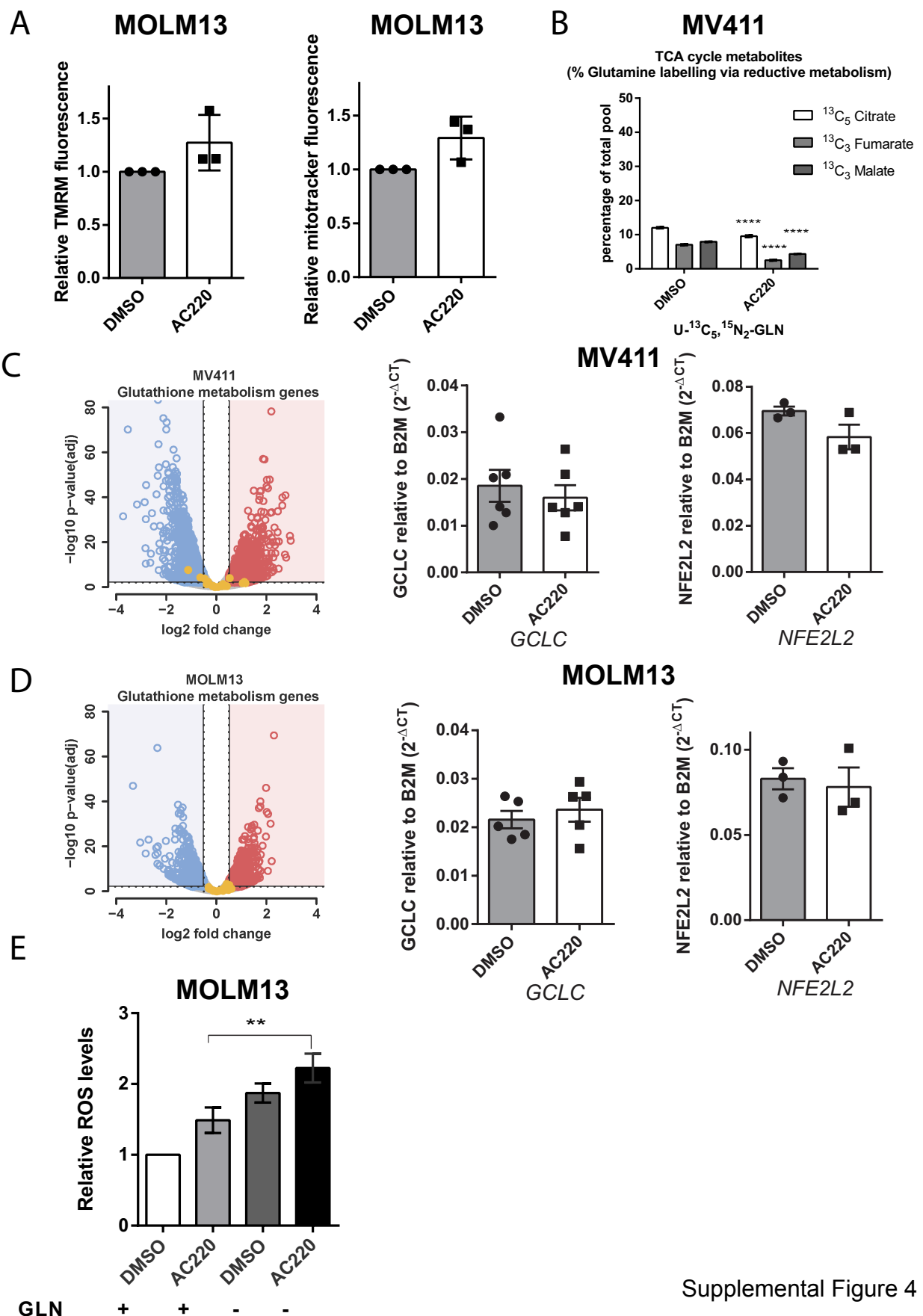
(A-C) GSEA analysis^{6,7} comparing gene expression profiles obtained from AML patient cells at diagnosis from 3 independent datasets (AML-TCGA, GSE6891, E-TABM1029) showing upregulation of glucose metabolism and TCA cycle and ETC genes in FLT3^{ITD} compared to FLT3^{WT} patients (NES, normalized enrichment score, FDR, false discovery rate). (D) Heat map showing relative expression levels for key genes involved in glycolysis, TCA cycle and ETC comparing FLT3^{ITD} versus FLT3^{WT} patients from E-TABM1029 dataset. (E-F) ECAR (E) and oxygen consumption rate (OCR) (F) in murine bone marrow cells transgenic for FLT3^{ITD} compared to their isogenic FLT3^{WT} counterpart (mean \pm s.e.m., n=3, glycolytic rate **** P<0.0001, maximal glycolytic capacity * P=0.0415, basal respiration ** P=0.0098, maximal respiration **** P<0.0001, two-way ANOVA with Bonferroni's multiple comparisons).



Supplemental Figure 3

Supplemental Figure 3 (Related to Figure 2): Effects of AC220 on FLT3^{ITD} cells proliferation and gene expression

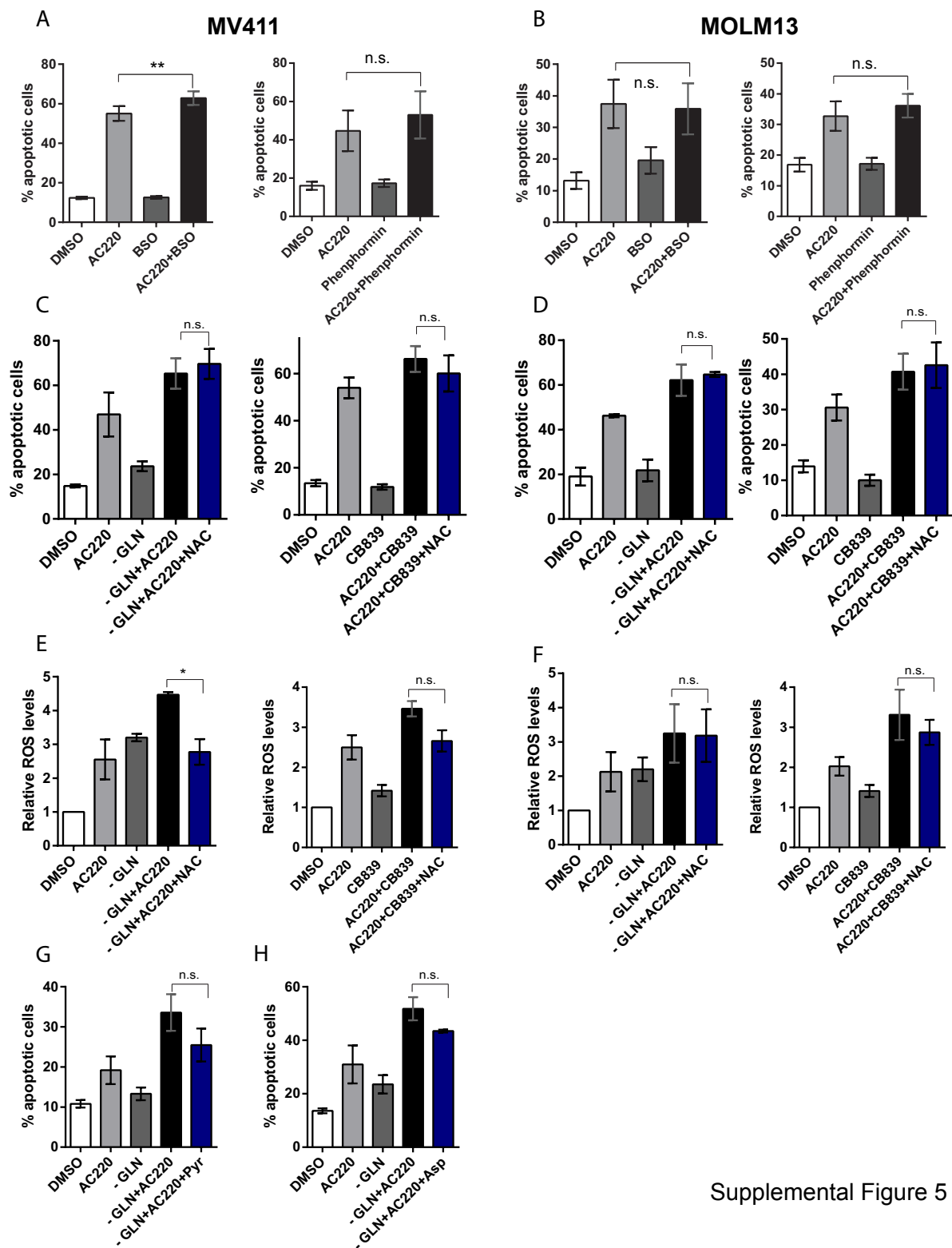
(A-B) Growth curves of FLT3^{ITD} mutated cells following treatment with AC220 1 nM or vehicle control (mean \pm s.e.m., MV411 n=14 and MOLM13 n=5). (C-D) Changes in expression by q-PCR in anaplerotic metabolism genes pyruvate carboxylase (PC) and pyruvate dehydrogenase E1 alpha subunit (PDHA1) and pyruvate dehydrogenase E1 beta subunit (PDHB) following treatment with AC220 1nM or vehicle control (mean \pm s.e.m., n=3, PC for MV411 *P=0.0469, for MOLM13 p=0.0244, two-tailed paired t-test. Not significant for PDHA1 and PDHB).



Supplemental Figure 4

Supplemental Figure 4 (Related to Figure 3): Extended data on the role of glutamine in supporting both mitochondrial function and redox metabolism following FLT3 tyrosine kinase inhibition

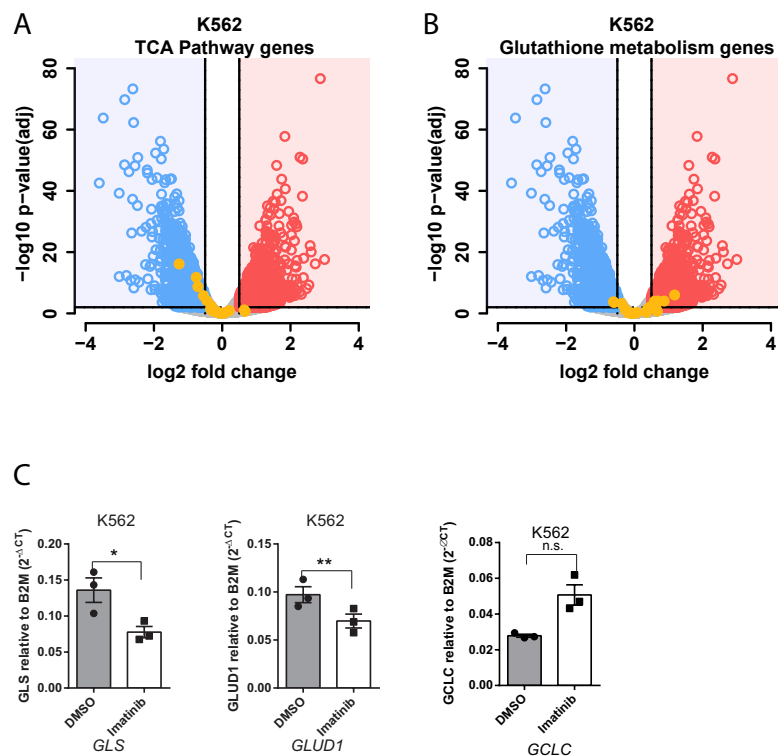
(A) Relative mitochondrial membrane potential (left, mean ± s.e.m., n=3, not significant), and relative mitochondrial mass (right, mean ± s.e.m., n=3, not significant) of MOLM13 cells treated with AC220 1 nM or vehicle control. (B) Percentage of total levels of TCA cycle metabolites labelled by U-¹³C₅, ¹⁵N₂-GLN through its reductive metabolism measured by LC-MS analysis in MV411 cells treated with AC220 1 nM or vehicle control (mean ± s.e.m., n=5, **** P<0.0001, two-way ANOVA with Bonferroni's multiple comparisons) (C-D) Volcano plot for gene expression changes by RNA-sequencing analysis of MV411 (C) and MOLM13 (D) cells treated as in (A) highlighting the minimal effects on genes involved in glutathione metabolism with q-PCR validation for the rate limiting gene in the production of glutathione, glutamate-cysteine ligase catalytic subunit (*GCLC*) (mean ± s.e.m., n=6, not significant) and the master regulator transcription factor of antioxidant response *NFE2L2* (mean ± s.e.m., n=3, not significant). (E) Relative ROS levels of MOLM13 cells treated with AC220 1 nM or vehicle control in the presence or absence of glutamine (mean ± s.e.m., n=8, ** P=0.0041, ANOVA with Tukey's multiple comparisons).



Supplemental Figure 5

Supplemental Figure 5 (Related to Figure 4): Single targeting of mitochondrial function and redox metabolism following FLT3 tyrosine kinase inhibition does not fully phenocopy the effects of GLS inhibition

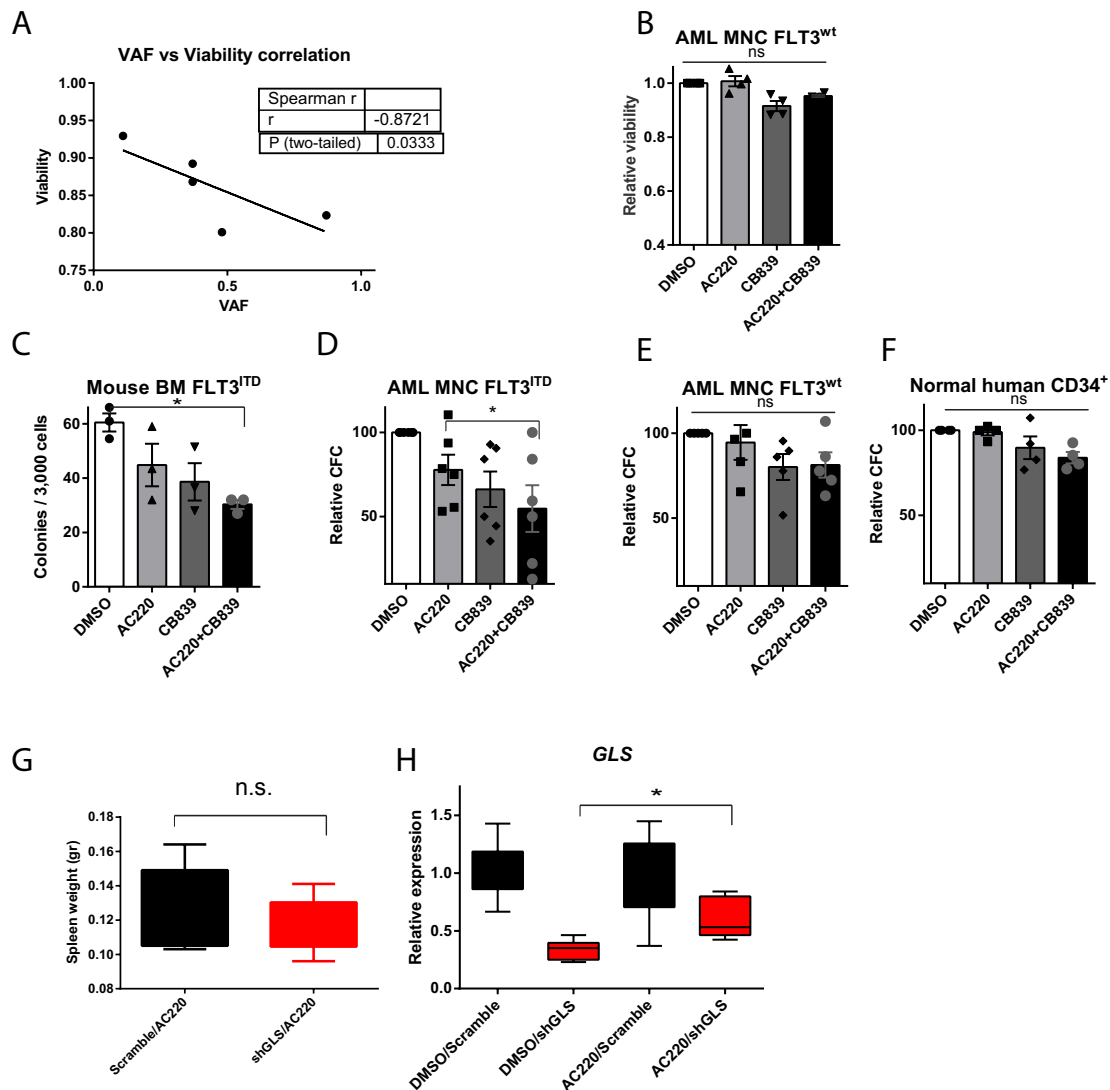
(A-B) Apoptosis in the FLT3^{ITD} cells MV411 **(A)** and MOLM13 **(B)** following treatment with AC220 1 nM, BSO 100 μ M or their combination (left panels, mean \pm s.e.m., for MV411 $n=15$, ** $P=0.0059$, for MOLM13 $n=4$, n.s., not significant, ANOVA with Tukey's multiple comparisons) or AC220 1 nM, Phenformin 2 μ M or their combination (right panels, mean \pm s.e.m., $n=3$, not significant, ANOVA with Tukey's multiple comparisons). **(C-D)** Apoptosis in the FLT3^{ITD} cells MV411 **(C)** and MOLM13 **(D)** following treatment with AC220 1nM with or without supplementation of glutamine (- GLN) and following N-acetylcysteine (NAC) treatment at 1.25 μ M (left panels, mean \pm s.e.m., $n=4$, not significant for NAC rescue, ANOVA with Tukey's multiple comparisons) or AC220 1nM, CB839 100nM or their combination and following NAC treatment at 1.25 μ M (right panels, mean \pm s.e.m., $n=5$, not significant for NAC rescue, ANOVA with Tukey's multiple comparisons). **(E-F)** Relative ROS levels in the FLT3^{ITD} cells MV411 **(E)** and MOLM13 **(F)** following treatment as in **(C-D)** (left panels, mean \pm s.e.m., $n=4$, * $P=0.0144$, for NAC rescue and not significant for NAC rescue, ANOVA with Tukey's multiple comparisons) (right panels, mean \pm s.e.m., $n=7$, not significant for NAC rescue, ANOVA with Tukey's multiple comparisons). **(G-H)** Apoptosis in the FLT3^{ITD} cells MV411 following treatment with AC220 1 nM with or without supplementation of glutamine and following pyruvate (Pyr) 1 mM **(G)** (mean \pm s.e.m., $n=5$, not significant for pyruvate rescue, ANOVA with Tukey's multiple comparisons) or aspartate (Asp) 10 mM supplementation **(H)** (mean \pm s.e.m., $n=4$, not significant for aspartate rescue, ANOVA with Tukey's multiple comparisons).



Supplemental Figure 6

Supplemental Figure 6 (Related to Figure 5): Extended data on the effects of Imatinib treatment and *GLS* inhibition in BCR-ABL positive cells

(A-B) Volcano plot for gene expression changes by RNA-sequencing analysis of K562 cells treated with vehicle control or Imatinib 2 μ M highlighting the minimal effects on genes involved in TCA cycle (A) and glutathione metabolism (B). (C) Changes in expression by q-PCR in glutamine metabolism genes *GLS* (n=3, *P=0.0342), *GLUD1* (n=3, ** P=0.0036), and glutathione metabolism gene *GCLC* (n=3, n.s.) following treatment of K562 cells as in (A-B) (mean \pm s.e.m. are shown, P values are calculated using two-tailed paired t-test).



Supplemental Figure 7

Supplemental Figure 7 (Related to Figure 6): Extended data on the effects of AC220 treatment and GLS inhibition in primary AML samples and *in vivo*

(A) Correlation between VAF for FLT3^{ITD} mutation of primary samples and their sensitivity to combination treatment. (B) Relative viability in primary FLT3^{wt} mutated AML samples treated with vehicle control, AC220 2.5 nM, CB839 100 nM or their combination (mean \pm s.e.m., n=4). (C) Relative colony output of mouse bone marrow FLT3^{ITD} positive cells following treatment with AC220 5 nM, CB839 100 nM or their combination (mean \pm s.e.m., n=3, * P=0.0211, between DMSO versus AC220+CB839, ANOVA with Tukey's multiple comparisons). (D-F) Relative colony output of primary FLT3^{ITD} mutated AML samples (D), FLT3^{wt} AML samples (E) and normal CD34⁺ cells (F) following treatment with AC220 2.5 nM, CB839 100 nM or their combination (for FLT3^{ITD}, mean \pm s.e.m., n=6, * P= 0.0296; for FLT3^{wt}, mean \pm s.e.m., n=5, ns; for CD34⁺, mean \pm s.e.m., n=4, ns, ANOVA with Bonferroni's multiple comparisons). (G) Spleen weight of mice transplanted with MV411 cells transduced with control "Scramble" shRNA (n=9) and GLS shRNA (n=8) following treatment with AC220 (box and whiskers showing minimum to maximum range, unpaired t-test, n.s.). (H) Relative expression levels measured by q-PCR of human GLS from hematopoietic tissue collected at death from mice transplanted with MV411 transduced with control "Scramble" shRNA and GLS shRNA treated respectively with DMSO or AC220 by oral gavage (box and whiskers showing minimum to maximum range, n=9 for DMSO and n=7 for AC220, * P= 0.0276, ANOVA with Bonferroni's multiple comparisons).